Calibration Procedures and the System of Data Acquisition and Monitoring for the Baikal Neutrino Telescope NT–200

presented by *S.I.Klimushin*

Institute for Nuclear Research, Moscow, Russia
e-mail: klim@pcbai10.lpi.msk.su

for the Baikal Collaboration

Abstract

The large deep underwater Neutrino Telescope NT–200 with 192 PMTs is presently taking data in Lake Baikal. This paper describes the basic procedures for calculation of the time and amplitude calibration parameters of its measuring system. A brief overview of the front-end electronics and triggering principles is given. The DAQ-system including a Transputer Farm and the Telescope monitoring capacities are reviewed.

1 Introduction

This paper discusses in more detail the topics which are usually incomplete in the general descriptions of the Baikal Telescope [1],[2]: the calibration procedures and their accuracies, the shore Data Acquisition (DAQ) system based on a medium scale but rather fast and reliable Transputer net and a Monitor system reflecting the operation of NT–200 in real time. A lot of attention has been focussed to the amplitude calibrations, in spite of only indirect use of the amplitude information for track reconstruction and neutrino event recognition through a set of special amplitude based cuts [4],[5].
This paper omits the description of the special experiments investigating the features of a smart photodetector *QUASAR-370* (consisting of big photocathode and small PMT [3]) which are being an important part of calibration procedures and have been described in detail in [2].

2 NT–200 Front-End Electronics and Triggering Modes

2.1 Svjaska System Module

All 192 Optical Modules (OM) of NT–200 are arranged in pairs being operated in coincidence (with a window width of 15 ns) and forming thus 96 measuring channels. The front-end electronics for each 2 channels (4 OMs) is provided in a separate electronics unit, the so-called *Svjaska System Module* (SSM) (in russian "svjaska" means a "bundle").
Fig.1 shows the scheme of the SSM for one measuring channel (one pair of OMs). The anode signals are sent to a local trigger board realizing a 2-level discrimination logic and coincidence

(for more details see [2]). The discriminator thresholds (being set with respect to the photoelectron scale of the big photocathode) are remotely adjustable to values between 0.1 – 10 p.e. and set typically to 0.3 p.e. In addition, through this board one has the possibility to switch off from the coincidence one OM from a pair (if necessary). The dynode signals are sent to a Q-T converter and summarized by an analog summator. One can set remotely the summator to a mode where the charge of the dynode signal will be taken only from one OM instead of both OMs of a pair (the first is just the case for the basic mode of NT–200 operation).
Thus, if both OMs of a given channel show a signal above threshold ($\approx$ 0.3 p.e.) within a time window (15 ns) the *local trigger* condition is generated and the output signal after Q-T conversion is sent to a *String Electronics Module* (SEM) and fed to TDCs digitizing the time (11 bit with a resolution 1 ns) and the time converted amplitude (10 bit) information. The length of this local trigger signal corresponds to the charge of the dynode signal and its leading edge defines the timing and is set by the earliest of the 2 OMs of a pair.
The Q-T converter can be operated in two remotely set modes: in the *standard* mode, when the amplitude digitizing TDC has a resolution of 1 p.e. (with dynamic range 1 – 1000 p.e.) and a *stretched* one with a resolution of $\sim$ 0.05 p.e. (dynamic range 0.05 – 50 p.e.).
Further components of the SSM are: a LED driver controlling the LED intensity and allowing to emulate "false" local triggers for test goals and a slow net *Communication Controller* (CC) driving the HV values of the small PMTs and all components of SSM being remotely controlled (discriminators, LED, Q-T converter). In addition, its programmable on-board generator is used to set the frequency of the LED pulses and "false" local triggers (within 1 – 1000 Hz).

2.2 Master and Test Modes

The logic of the trigger formation for NT–200 is explained in Fig.2. Upon receiving a local trigger from a given channel, the SEM (handling 6 channels) stretches this signal by a factor of 70 and starts the digitization of time and amplitude in the corresponding TDCs within an interval of about 2 μs. For the *Master Mode* (which is the default Mode of operation) the results of time and amplitude code measurements will be reset if during the period of the digitization the stop signal from the *Detector Electronics Module* (DEM) confirming the fulfillment of a trigger condition (and stopping timing signal formation) will not arrive. If this confirmation took place, the resulting TDC content is shifted to the FIFO of the Slave Data Controller (SDC) positioned in the SEM (with the addition of the information about channel and event number) and further transmitted to shore via a fast data link. The Master Mode is the basic Mode of NT–200 data taking, which aims to record the local triggers resulting mainly from muon-like events. The stop signal is formed by the requirement of $\geq m$ local triggers within a time window of 500 ns (so-called muon trigger). The threshold value m of the DEM triggering discriminator can be set from shore to values between 1 and 7. The basic NT–200 muon trigger is set to $m = 4$.
In addition to the Master Mode a special *Test Mode* is implemented for calibration reasons. In this case the forced reset of TDCs after 2 μs is canceled and the stop signal of DEM confirmation is produced almost always by a generator running in the DEM (the period T_s of these synchropulses is 1400 ns with a high accuracy). The origin of the local triggers is defined by the corresponding calibration regime and may result from pulses of the CC generator (emulating local triggers or firing the LED) or by OM noise pulses being a superposition of PMT dark current and luminescence of water. Taking into account that the capacities of the fast data transmission line are restricted to 6 kB/s and that counting rate of local triggers is rather high (typically 100 – 300 Hz for the noise pulses and 1 kHz for CC generator), the results of TDC

digitization are stored in SDC memory as amplitude and time distributions and read from shore only after finishing a given calibration regime.

3 Calibration Parameters of NT–200

Here we will primarily investigate the amplitude and time calibration procedures for the full Telescope resulted from the Standard (Master Mode) and Calibration (Test Mode) Runs. Calibration of NT–200 means basically the determination of characteristic parameters for the transformation of the raw digitized TDC codes into "physical" values of times [ns] and amplitudes [p.e.]. In order to measure the majority of these parameters, the data taking of NT–200 is interrupted every 5 days for *Calibration Runs* being performed in the Test Mode. The duration of the Calibration Run depends on the required statistics in the distributions and is usually about 4 hours.

3.1 Amplitude

The transformation of the amplitude from 10-bit digitized TDC code A into photoelectron value a [p.e] for a given channel i is done by

$$a_i = (A_i - P_i) \cdot \alpha_i \tag{1}$$

using 2 calibration parameters: the *pedestal* value P_i and the scale factor for amplitude digitization α_i.

The pedestal distributions (both for the standard and stretched modes of the Q-T converter) are obtained through the startup of the CC generator (1 kHz) when emulating "false" local triggers. Their typical shapes are shown in Fig.3. The mean values of these distributions calculated within 4σ-area around the peak position define the standard (P) and stretched (P_{str}) pedestals. The widths σ of these distribution for 80 % of channels range between $0.4 \div 0.6$ for the standard pedestals and $2 \div 5$ for the stretched ones.

The *amplitude scale factors* α can be determined via two main methods. The first one is based on the amplitude distributions of multi-photoelectron pulses from different sources of light (LED or laser). The average number of photoelectrons N_{pe} is derived from

$$N_{pe} = \frac{(\overline{A} - P)^2}{D} \cdot (1 + {\delta_1}^2) \tag{2}$$

with P being the pedestal and $\overline{A}$ and D being mean value and dispersion (σ^2) of the distribution, respectively. ${\delta_1}^2 = (\sigma_1/A_1)^2$ represents the relative dispersion of the charge distribution of a PMT single-photoelectron signal (with σ_1 and A_1 being width and mean value of this distribution, respectively). Typically $(1 + {\delta_1}^2)$ has a value about 1.2. The ratio $N_{pe}/(\overline{A} - P)$ gives the scale factor α.

The standard Calibration Run performs a calibration of each individual OM (i.e. with the 2 OMs of a pair switched sequentially to the summator of Q-T converter) with the help of LEDs which are located in each SSM. The typical LED multi-photoelectron distributions are shown in Fig.4. For the isolation of the LED-part of these distribution from the area resulted primarily from the muon-like events detection the region within 4σ around LED-peak is taken. Our case (for channel 49) results in N_{pe}=46 p.e. and α=1.27. We note that the Gaussian fit may show a small assymetry of the multiphotoelectron distribution even for values ≈ 50 p.e. (lower picture in Fig.4).

The error of the α calculation is defined primarily by uncertainties in the knowledge of ${\delta_1}^2$ and by the accuracy of the LED-area isolation which influences the dispersion value D. It is estimated to 10 – 15 %.
By special Calibration Runs where the charge distributions are accumulated for a set of the different intensities of LED-flashes one may examine the *linearity* of the dependence $N_{pe}(\overline{A})$ defined by expression (2). Fig.5 sketches the typical behaviour of this dependence for different channels conditionally divided into "linear" and "nonlinear". About 70 % of the operating channels have shown a good linearity (within 10 % percent) up to 300 p.e.
Another way of an independent determination of the amplitude scale factor α consists in the analysis of the *noise* PMT spectrum produced for the stretched mode of the Q-T converter. The accumulation of this spectrum for every OM of NT–200 (Fig.6) is included into the standard Calibration Run. It yields to equation of the α definition

$$1\ p.e. = \frac{(A_{1pe} - P_{str})}{K_{str}} \cdot \alpha \tag{3}$$

where A_{1pe} is the charge value corresponding to 1 p.e., P_{str} and K_{str} are the pedestal in the stretched mode and stretching coefficient, respectively. As A_{1pe} we took the amplitude code corresponding to the most probable value of the noise spectrum. Our case ($K_{str} = 20.4$ and $P_{str} = 195$ for channel 49) gives $\alpha = 20.4/(210 - 195) = 1.36$ which is in a good agreement (7 %) with the result of the LED-method.
The analysis of the left edge of the 1 p.e. peak of the stretched noise distribution allows the estimation of the established *threshold* value. Generally the left edge has a quasivertical break, the middle of which is taken as the threshold value. In the cases when the slope of the left edge doesn't change and the threshold is shadowed (mainly by the stretched pedestal dispersion) the combined comparison of 2 noise spectra with working and low thresholds is implemented (Fig.7). Our case results in the threshold value $(202 - 195) \cdot 1.36/20.4 = 0.47$ p.e. The accumulation of the noise spectra with low thresholds are also included into the standard Calibration Run.
The α values can be changed by the high voltage selection for the small PMT until one photoelectron corresponds to one amplitude channel. The threshold values are controlled by the CC and set to ≈ 0.3 p.e.
The stretching coefficients K_{str} for the every channel could be calculated after retransformation of the corresponding differential amplitude spectra which have been taken from the Standard NT–200 Runs via Master Mode with $m = 4$ at standard and stretched modes (Fig.8) into *integral* spectra. In that case K_{str} is given by the ratio A_{N_str}/A_N, where A_{N_str} and A_N are the amplitude codes (without pedestals) corresponding to the same statistics $N(\%)$ at the integral spectra for the standard and stretched modes respectively (Fig.9). Generally $N \approx 10\%$ gives the resulting K_{str} ranged for NT–200 within 18 – 23. This method allows to estimate K_{str} with an accuracy of about 5 %.

3.2 Time

The response time t_i (in ns) of a channel i with respect to the time of the stop signal of the Detector Electronics Module (DEM) confirmation is determined by two calibration parameters,

$$t_i = \beta_i \cdot T_i + \Delta t_i \tag{4}$$

with β_i being the scale factor for the time digitization, Δt_i (in ns) being the individual shift of channel i (resulting mainly from the regular time delays because of the different lengths of cables

linking SSMs and SEMs) and T_i the measured TDC time code for channel i.
For the Test Mode of NT–200 the TDCs are started by test-, LED or noise pulses (with typical frequencies 100 – 1000 Hz) and stopped by DEM generator synchropulses with a period $T_s = 1400$ ns (Fig.2). So, the probabilities of digitizing of every code within the time window T_s should be equal and result in an uniform distribution of time code. The deviation from the uniformity may be caused by a differential (local peculiarities) or integral nonlinearity of the corresponding SEM time channel.
These distributions for the full Telescope are accumulated simultaneously (together with the amplitude distributions) for all stages of the Calibration Run. The typical shape of the time code distribution (has been stored in LED-regime of Calibration Run) is shown in Fig.10. The end points of the plateau K_{min} and K_{max} are taken at half of the plateau level. They are determined typically with an accuracy of 1 code (1 ns for a 10 bit TDC). The β_i are given by $T_s/(K_{max} - K_{min} + 1)_i$ and the widths σ_t of these distribution (in ns) by $\sigma \cdot T_s/N_{tot}$ (where σ is the standard deviation from the mean level and N_{tot} is the total number of entries). For more than 90 % of the operating channels of NT–200, σ_t is less than 1 ns what reflects the linearity for the majority of time channels.
The individual time shifts Δt_i are determined with the help of 2 calibration nitrogen lasers being automatically started in turn during Laser Runs being performed in the Master Mode. For the *"fiber"* laser, the light pulses of less than 1 ns width are guided via optical fibers of equal length to the OMs, with one fiber illuminating one OM pair (see [3]). For the *"water"* laser arranged 20 m below the array at the central string, the light propagates directly through the water.
The light of each laser is shifted from 337 nm to 475 nm by a dye laser. An attenuator enables to change continuously the intensity of the flashes. During the Laser Run both lasers perform sequences of 200 shots (with periodicity of 9.1 Hz) with 5 different intensities ($5 \cdot 200 = 1000$ pulses). The required number of such sequences is set from shore and is usually 3 – 7. A laser pulse generates a "laser" event with typically most of the channels firing (Fig.11.a). With special cuts one can select the events corresponding to a given laser intensity (Fig.11.b) then estimating (by using (2)) N_{pe} and the amplitude scale factor (but for rather small statistics). The ratio between the number of hits of a given channel and the total number of "laser" events within the selected sequence gives the channel efficiency (Fig.11.c).
The time shifts could be estimated from (4) as the solution of the system of linear equations:

$$\Delta t_i - \Delta t_j = \beta_j T_j - \beta_i T_i + \delta t_{ij} \tag{5}$$

where $\delta t_{ij} = t_i - t_j$ is the time difference (in ns) between channels having number i and j. By default, δt_{ij} is 0 for a fiber laser and equals $(R_i - R_j)/c$ for a water laser (where R_i and R_j are the distances from the laser to the corresponding channels and $c = 0.2254$ m/ns).
Fig.11.d shows the time difference distribution for a Laser Run between two channels which have been seen the average charge of 63 p.e. and 22 p.e. (fiber laser sequence # 1). The width of this distribution is 1.9 ns ($FWHM = 4.5$ ns), but the peak position is determined with an accuracy better than one ns.
We observed a drift in the Δt_i values over several months, presumably due to changes in the speed of light in the fiber under long-time pressure or water diffusion. These small effects can be corrected a posteriori by reconstructing muon tracks and requesting an average time residual like that observed in MC calculations [2]. The overall accuracy of time shifts definition (after MC tuning) is about 2 ns.

4 Data Acquisition System of the Shore Station

When designing the shore station of data acquisition of the Baikal Neutrino Telescope (from the pilot arrays to NT–200) a top priority was given to its reliability and the simplicity of its handling. Finally the preference was given to a DAQ-system based on a robust and almost maintenance free configuration consisting of 3 PCs (running under DOS) and a multiprocessor Transputer Farm [6]. Fig.12 shows the sketch of the NT–200 shore station (as well as a part of the underwater electronics) where the main components are outlined below.

- The **Host PC** carries out the following tasks:
  - Full control of the net of slow Communication Controllers (CC) (based on Intel-8085 micro-processor) through the shore modem and underwater commutator unit. All parameters can be set from the Host PC: in the Svjaska System Module (SSM) (HV for the small PMTs, discriminator threshold on QUASAR tubes, LED driver and Q-T converter states, etc.), in the String Electronic Modules (SEM) (Monopole System states, Master/Test Mode setting) and in the Detector Electronic Module (DEM) (muon trigger dicriminator threshold, World Time counter reset, start/stop of Master/Test Mode). In addition, this net is used for the polling of Check Point tables of each SSM local trigger board containing the counting rates of the QUASAR tubes, the small PMTs, the local triggers and their logical combinations. This polling is performed every 2 minutes. The average rate of data transmission through the slow CC net is about 100 B/s.
  - Management of the fast Data Controller System being a net of 1 shore Master (MDC) and 16 underwater Slave Data Controllers (SDC), one per every SEM. This system is based on Zylog-80 micro-computers and may transmit data up to 6 kB/s.
  - Steering of the different Runs of NT–200 data collection (Standard, Laser, Calibration). During the start of a Run, the nets of slow and fast controllers are tested and tuned, what is reflected (together with SSM states) in the dynamic state record of the Telescope.
  - Data storage in real-time format using a large set of error and informational messages. The different types of data (after their recognition and preprocessing by the Transputer Farm) are stored in the common files and labeled by corresponding record pointers (data from Master and Monopole Systems, Check Point tables, Local Trigger System (LTS) data). The on-line text Run-book is produced automatically.

  The codes of the Host PC software are written in C.

- The **Transputer Farm** is the heart of DAQ-system and performs the event building, raw data preprocessing and preliminary error and quality analysis. By means of Telescope run-time supervision the behaviour of its elements is checked on-line in the form of a large set of monitorograms and histograms (for more details see section 5). The codes of Transputer software are written in C++ using a special preprocessor enabling the parallel tasks running [6].

- The **Monitor PC** serves as powerful graphics real-time display using HBOOK-HPLOT CERN program libraries. The user can inspect about 2000 different distributions. All of them are back-uped after the stop of a Run and form thus the full on-line Run-passport.

The Monitor PC allows to include user subroutines for the on-line data analysis up to track reconstruction. The codes of Monitor PC software are written in protected-mode FTN 77.

- The **Service PC** supports on-run management of the CC based system of Power Supply (PS) equipment of NT–200 consisting of 8 PS-boxes (0.6 A, 480 V of input PS per each string) as well as the handling of the environmental underwater arrays of NT–200: Hydroacoustical System of Coordinates Measurement (HASM), the Hydrological station of the water temperature and current measurement, the special device to measure in-situ the optical properties of water medium.

The clocks of all PCs are being synchronized via Global Position System (GPS) with an accuracy about 0.1 ms. The INTERNET link with the outer world is managed through a satellite antenna which is connected to a SUN-station.
The typical counting rate of muon triggers for the master condition m=4 is 13–14 Hz what leads together with the data from Monopole and Local Trigger System [3] to a data stream $\approx$1 kB/s or $\approx$ 70–80 MB per day. The data are stored without any cuts to 8mm EXA-byte tapes (2.3 GB) and then rewritten to a set of CDs. The typical duration of a Standard Run of data acquisition is 10–12 hours. The efficiency of data taking for NT–200 is close to 90 %. The Shore Station system is robust, reliable and comfortable. It is usually handled only by 1 shift person.

5 Transputer Farm

The Transputer Farm is sketched in Fig.13. It consists of 10 RISC-processors with RAMs (Transputer Modules (TRAM)) positioned in 2 Link Multiplexor Modules (LIM). Each LIM contains 5 TRAMs where 1 of them is the *Root* being responsible to the subnet booting, configuring and buffering. Each TRAM can be connected with 4 other ones. Both LIMs are positioned in a VME-sized crate with a Master Data Controller (MDC) realizing the protocol of NT-200 data collection and being linked with the data receiving TRAM T3 of LIM1 through the fast port INMOS C011.
LIM1 is a *Server* providing preprocessed data to the Host PC and a *Monitor* LIM2. The data preprocessing consists basically of the clusterization into common events of the mixture of odd data packets from measuring channels by means of the event number pointers. TRAM T2 of the Server LIM1 runs the event building as well as acquires data coming from the Monopole System and the LTS. All preprocessed data are guided to the Root TRAM of LIM2 which distributes them between TRAMs being responsible for time (T1), amplitude (T0), Monopole and raw channel data (T3) histogramming. The Root TRAM of LIM2 is performing the event histogramming (hit multiplicity distribution...). The last TRAM T2 in the Monitor LIM2 processes LTS and Check Point data. The Check Point tables, containing counting rates from the local trigger boards of SSMs are sent to LIM2 through the Root TRAM of the Server LIM, which handles the protocol to the Host PC. All the TRAMs of LIM2 are performing parallel tasks.

6 Monitor Picture Gallery

The Monitor PC is linked to the Transputer Farm via the Root TRAM of LIM2 and takes the corresponding histogram on request. In the following we show for reasons of illustration some of the 2000 monitorograms.
Fig.14 shows the channel abundance distribution for NT-200 after the first week of data taking as

a typical sample of a raw channel data monitorogram. The "holes" correspond to channels being out of order or operating in a single-OM mode, with high threshold and without coincidence (about 10 % of channels). The "peaks" are formed by upward faced channels. Fig.15 shows the distribution for the different combinations of time differences between channels at the upper half part of the central string. The calibration time scale factors are sent to the Transputer Farm from the Host PC. This is a typical sample of a time monitorogram.
Fig.16 gives the real time behaviour of counting rates for the Check Points of a given SSM. The stability of the operation for all 4 OMs of this SSM during a long run-time (about 16 hours) is quite good.
Fig.17 illustrates the more complicated analysis being performed by the Monitor PC with the Local Trigger System data (LTS). LTS represents a supplement for Monopole System [1] giving counting rates of all measuring channels (local triggers) every 0.8 s. The monitor titled *Av(Rate)* shows the averaged counting rates of local triggers for 10 SEMs within the run-time. Most of them lay between 100 and 300 Hz. The monitors *Sig(Rate)* and *Sig(Nhit)/SigPoisson* display LTS standard deviations and their ratios to Poissonian expectations, respectively. The majority of channels shows a Poissonian behaviour of noise (ratios are $\approx$1) and only a few of them deviate by more than a factor of 2. The last monitor titled *Ratio Average/Reference* shows the ratio of the current LTS average counting rates to those kept as Reference from precedent Run(s). Thus one can follow longterm changes of local trigger counting rates.
We emphasize that the on-line Telescope monitoring is extremely important to check the detector performance during the deployment process as well as to guide the shift personal during normal data taking.

7 Conclusions

- The majority of the calibration parameters are measured by "standard" Calibration Runs in the Test Mode performed every fifth day. The scale factors of the amplitude and time digitizing can be defined with accuracies 10–15 % and 1 ns, respectively. The linearity of amplitude measuring system can be checked with LED or laser light pulse sources and described by corresponding dependences.

- The Standard Runs of NT-200 data taking give important calibration information (i.e. stretching coefficients). The Laser Runs performed after the Calibration Runs (once per 5 days) provide the individual time shifts with an accuracy $\approx$2 ns after MC corrections and track reconstruction.

- The Transputer net based DAQ system of NT-200 allows data taking with high efficiency and reliability. Long Runs (10–12 hours) are feasible, only one on-duty person can handle the shore station.

- The Transputer based Monitor system provides full on-line supervision of the performance of the Telescope.

References

[1] I.A.Belolaptikov et al., Astroparticle physics, 7 (1997) 263-282

[2] R.I Bagduev et al., The Optical Module of the Baikal Deep Underwater Neutrino Telescope. preprint DESY 98-091 (1998) (to be published in NIM)

[3] S.I.Klimushin, The Lake Baikal Experiment: Status Report, This workshop

[4] I.A.Belolaptikov, Reconstruction of muon tracks..., This workshop

[5] Zh.-A.M.Djilkibaev, Search for nearly vertically upward moving muons..., This workshop

[6] H.Heukenkamp et al., A Transputer Based Data Acquisition System for the Baikal Neutrino Telescope, Informatik Aktuell (Springer, Berlin, 1994) 297

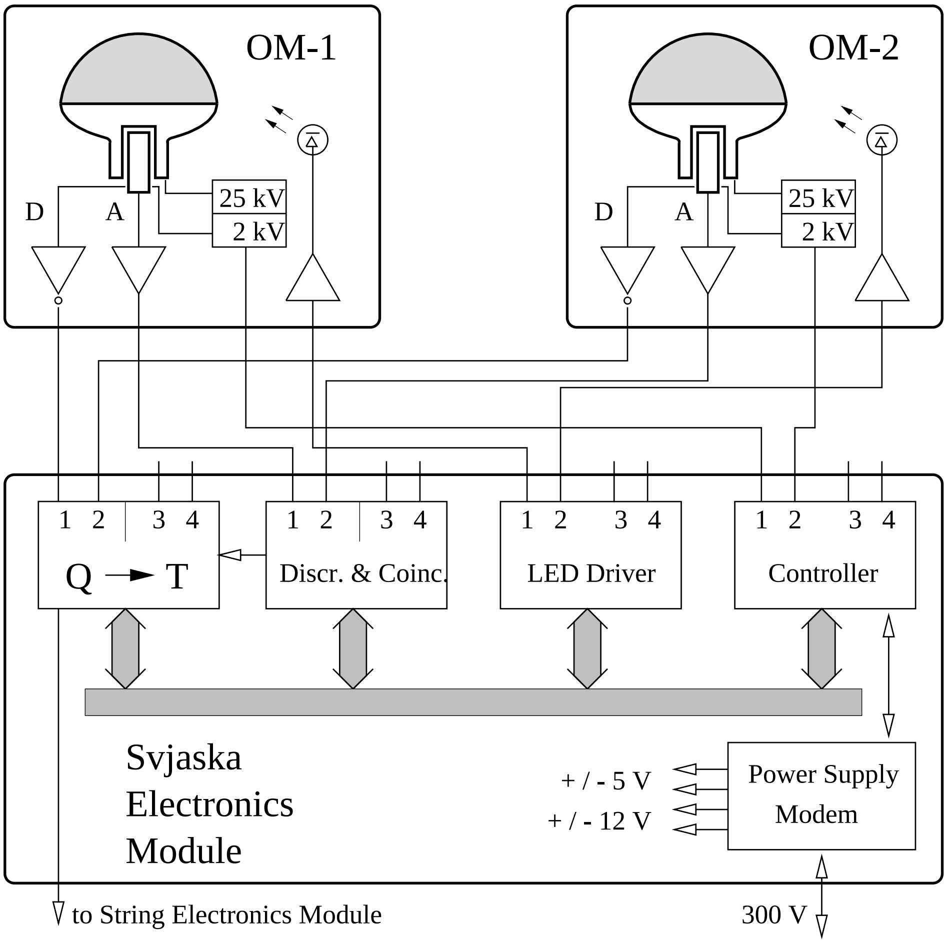

Figure 1: Sketch of the Svjaska System Module with 2 pairs of OMs (only 2 PMTs belonging to the first pair are shown).

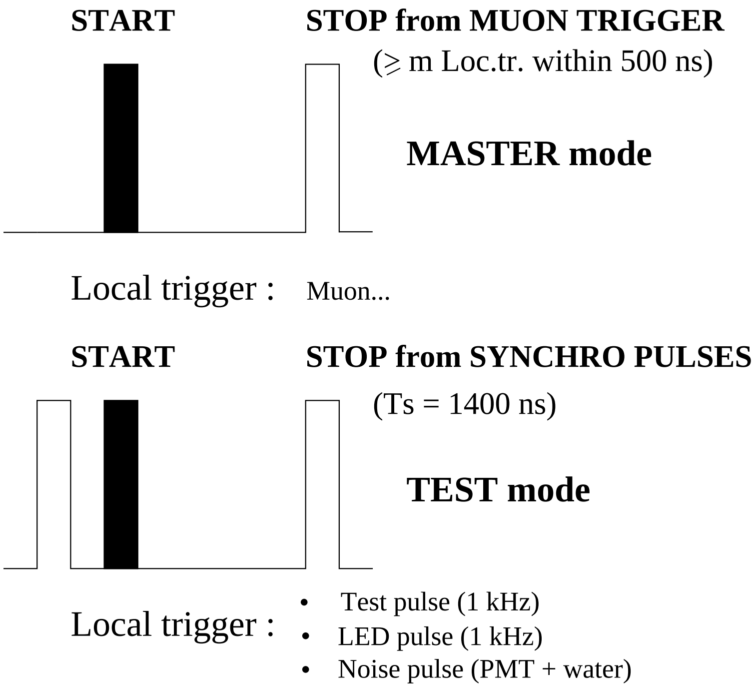

Figure 2: Trigger principles of Master and Test Mode.

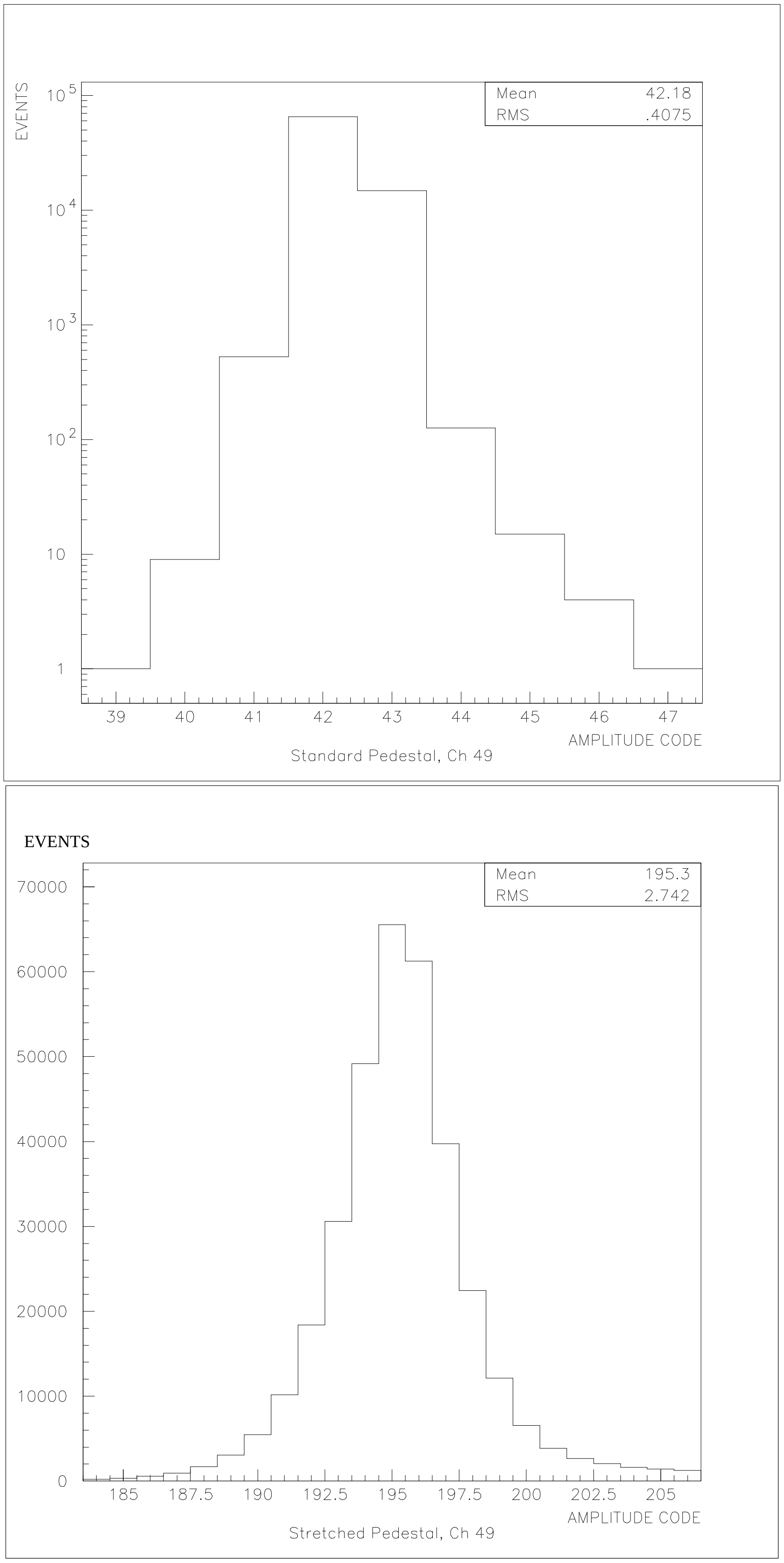

Figure 3: The pedestal distributions for the *standard* (upper picture) and *stretched* (lower picture) modes of Q-T converter. The stretched pedestal distribution is shown for the 4σ-region around the peak.

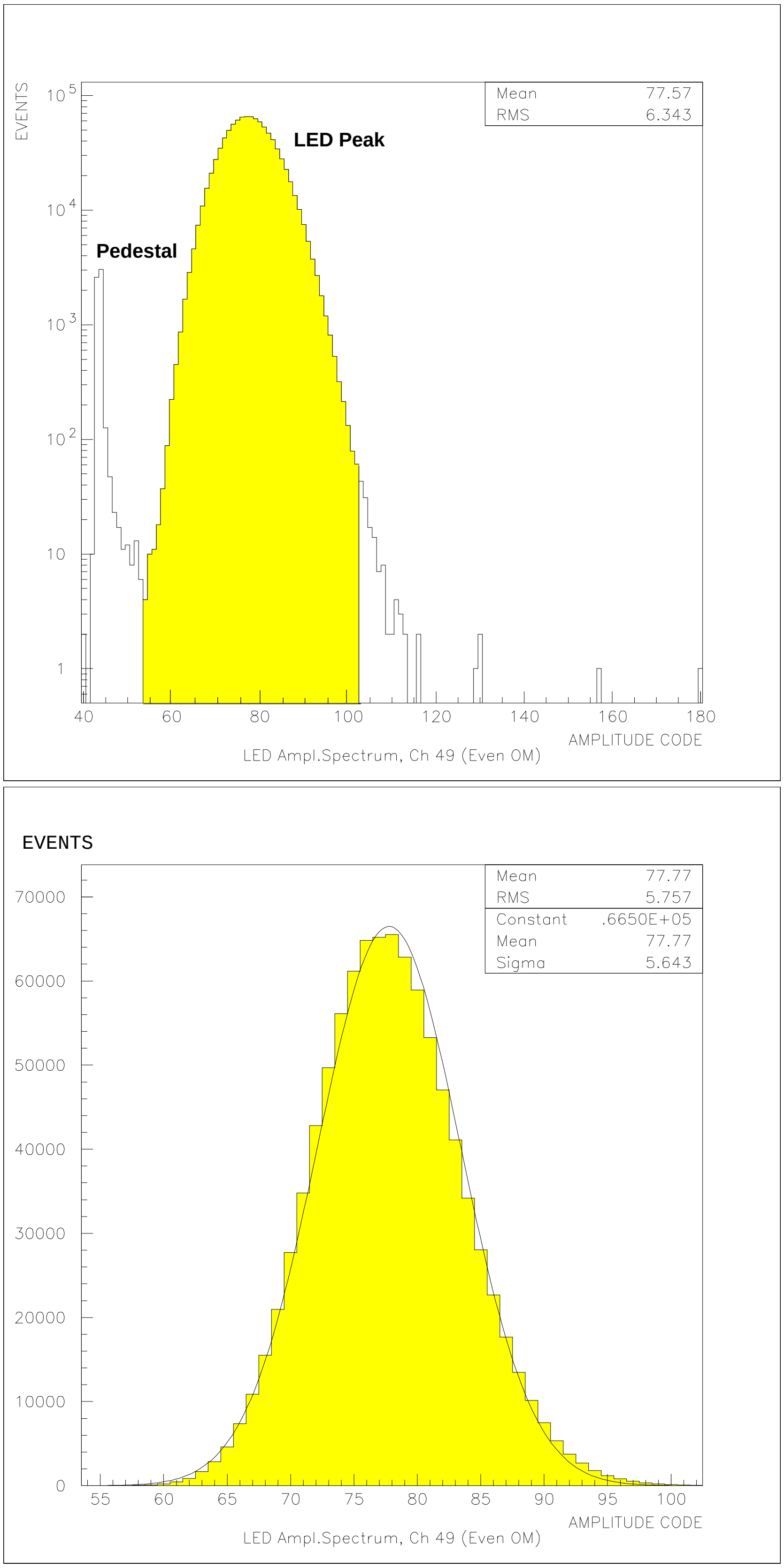

Figure 4: The amplitude distribution for multi-photoelectron LED-pulses. The upper picture shows the whole distribution with the hatched area corresponding to the 4σ-region around the LED-peak. This area is shown separately in the lower picture with a Gaussian fit (linear scale).

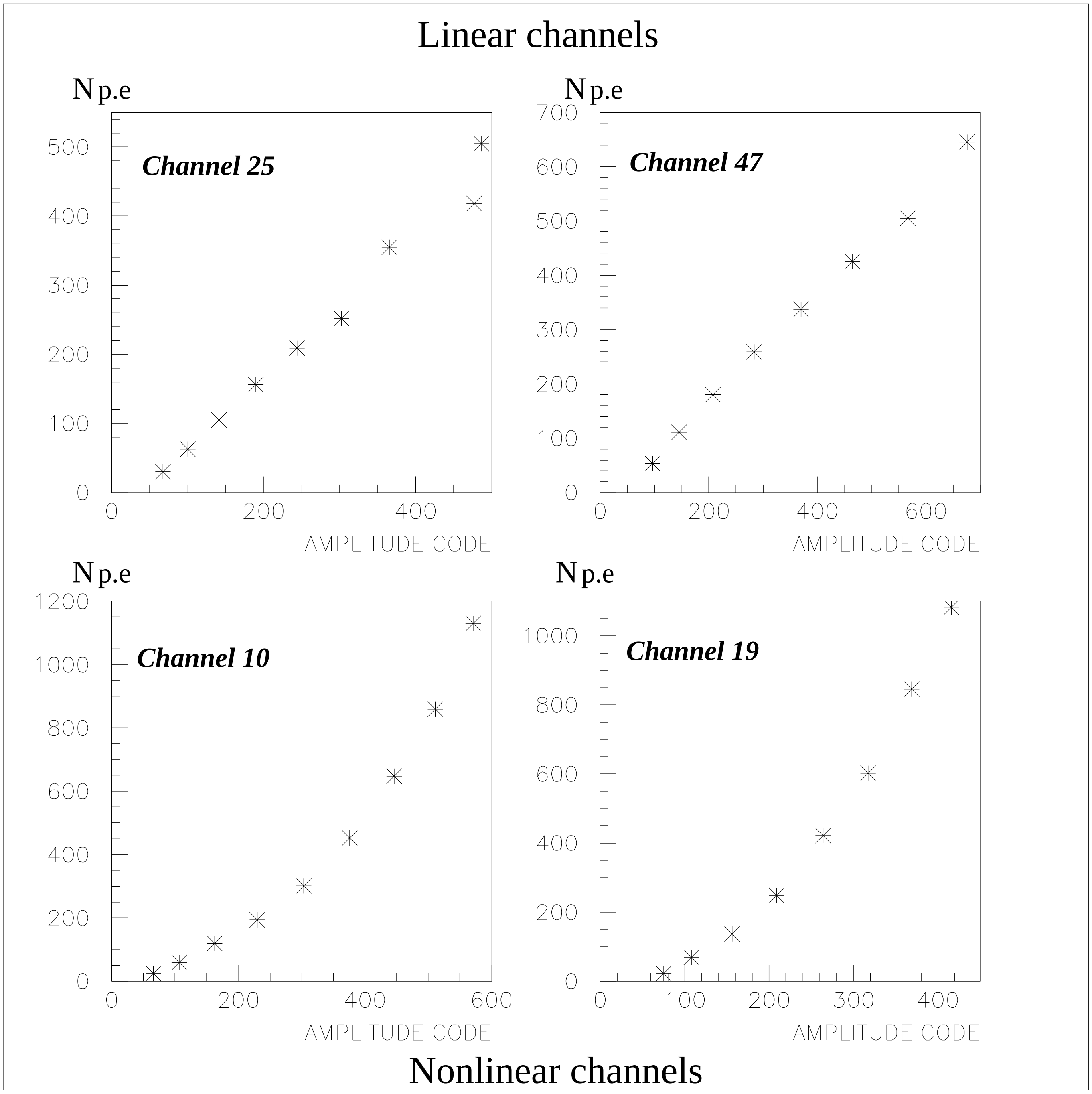

Figure 5: The dependencies of the average multi-photoelectron charge N_{pe} vs mean amplitude code (with pedestal values) illustrating the *linearity* of amplitude measurements. The distributions are resulted from the different intensities of LED-flashes.

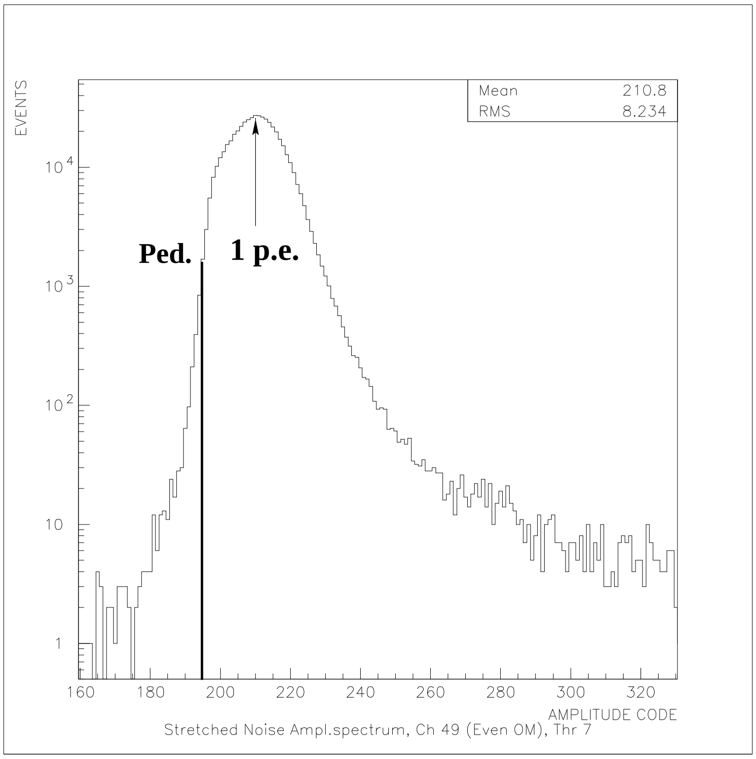

Figure 6: The noise PMT amplitude spectrum for the stretched mode of the Q-T converter. The positions of pedestal and single-photoelectron peak are shown.

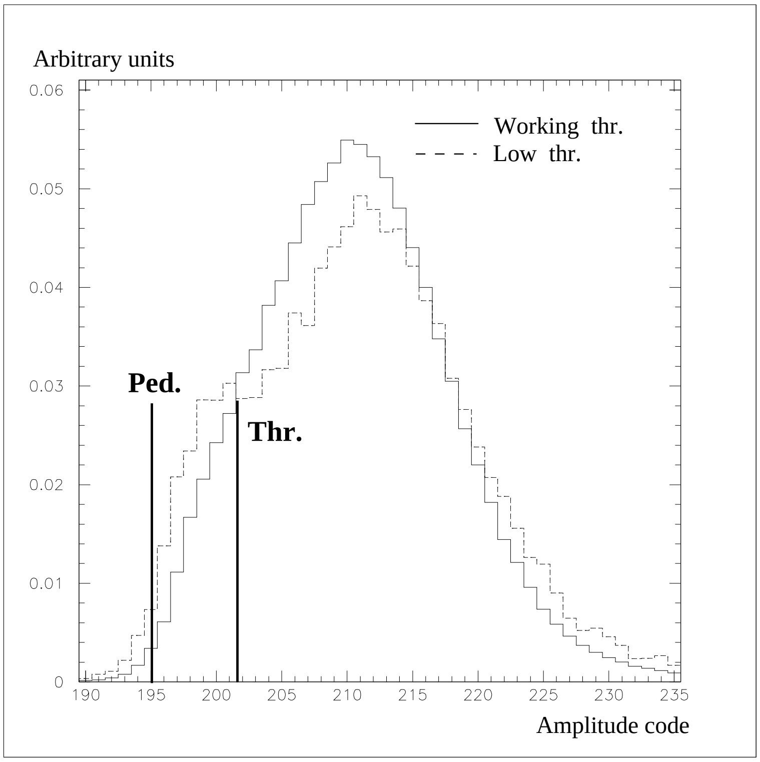

Figure 7: The stretched noise PMT spectra have been measured with the *working* (solid line) and *low* (dashed line) discriminator threshold. The distributions are normalized to the same area. The value Thr was taken as result for working threshold.

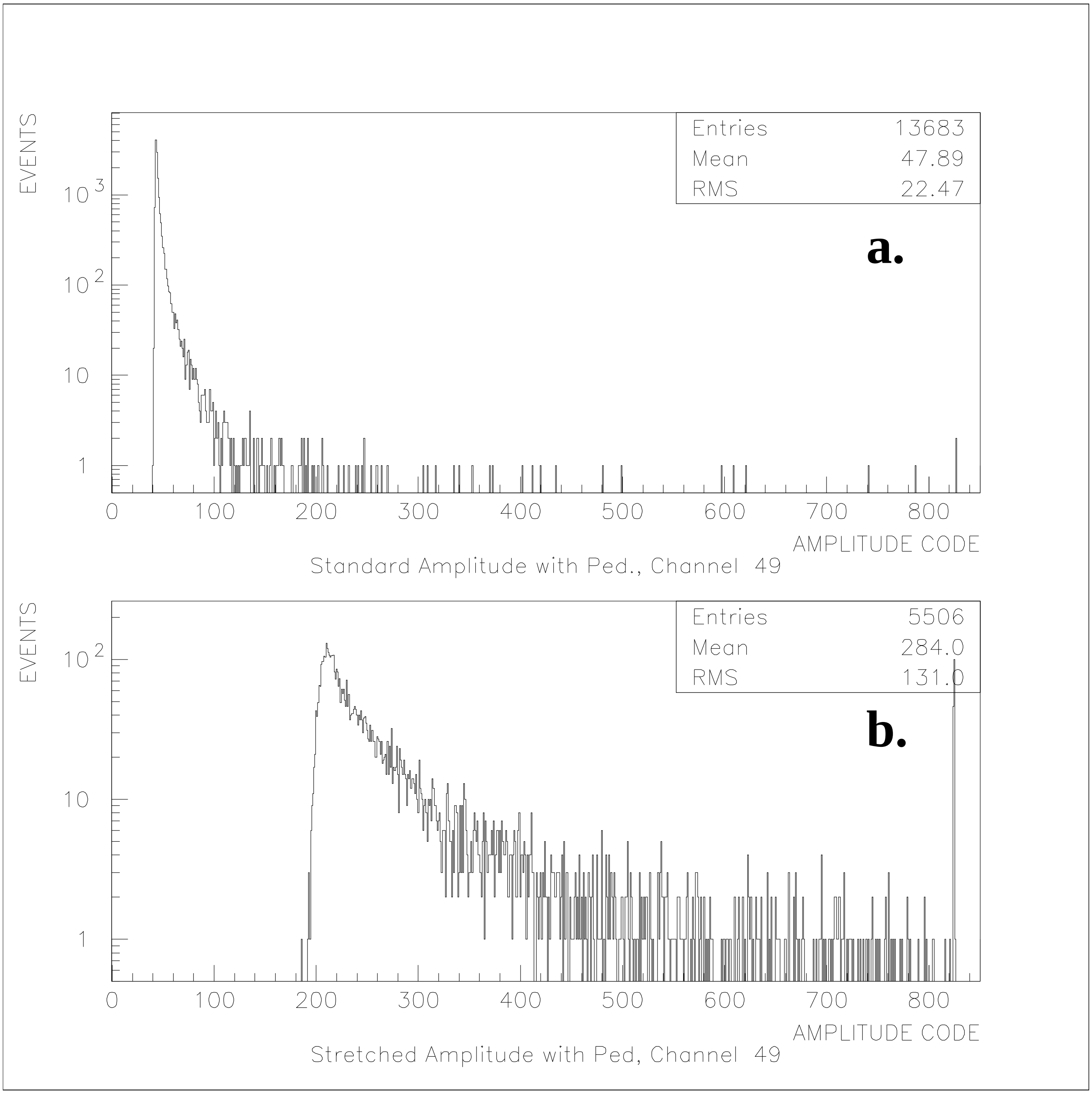

Figure 8: The *differential* amplitude spectra have been measured from Master Mode Runs with the standard (top) and stretched (bottom) modes of Q-T converter. The amplitude codes are with pedestals.

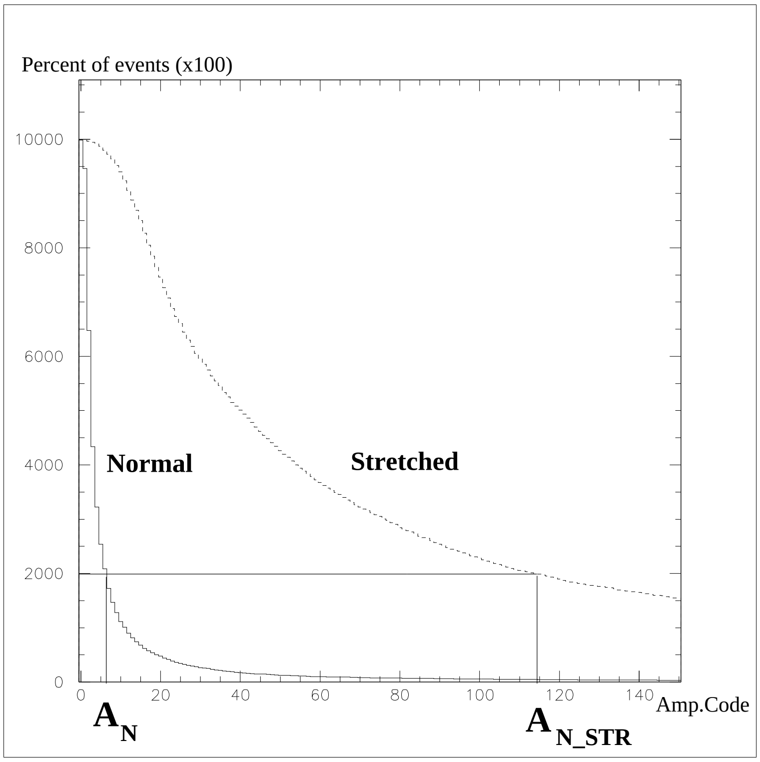

Figure 9: The *integral* amplitude spectra for the standard (normal) and the stretched mode of the Q-T converter (the corresponding pedestal values were subtracted). The values A_N and A_{N_STR} correspond to 20 %.

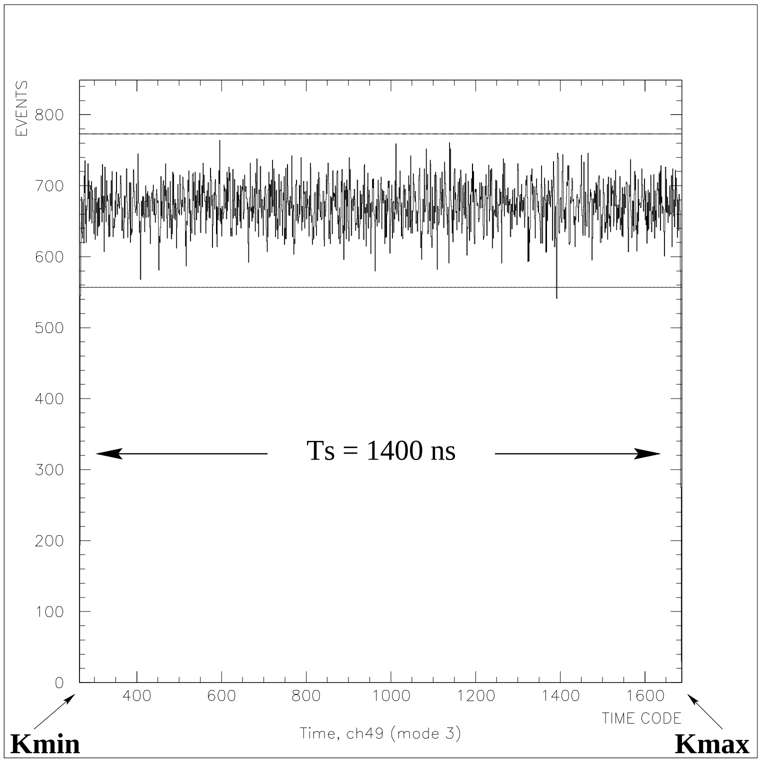

Figure 10: The typical uniform distribution of the time codes for the Test Mode. The 4σ corridor around the mean level is shown.

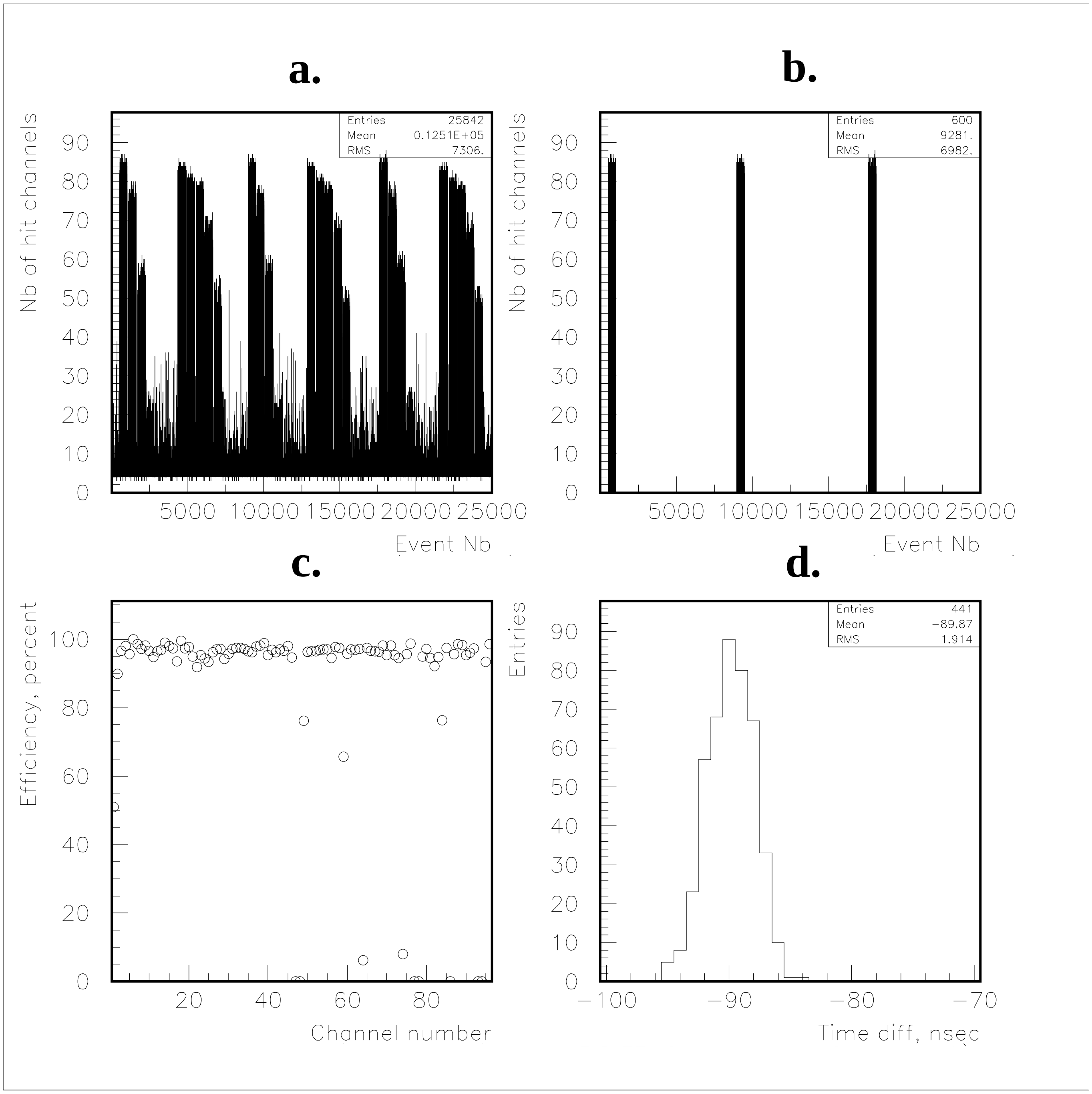

Figure 11: A set of distributions for a *Laser Run* of NT–200. **a)** The number of hit channels in a event vs the event number. Three sequences of *fiber* and *water* laser shots are shown. Each sequence consists of 200 shots which are repeated 5 times with decreasing intensity - first firing only the fiber laser and then only the water laser. **b)** The same after selection of only the most intense 600 shots of the 3 fiber laser sequences. **c)** The channel efficiencies from 3 fiber laser sequences with highest intensity. **d)** The distribution of laser light arrival time difference for channels 41 and 49.

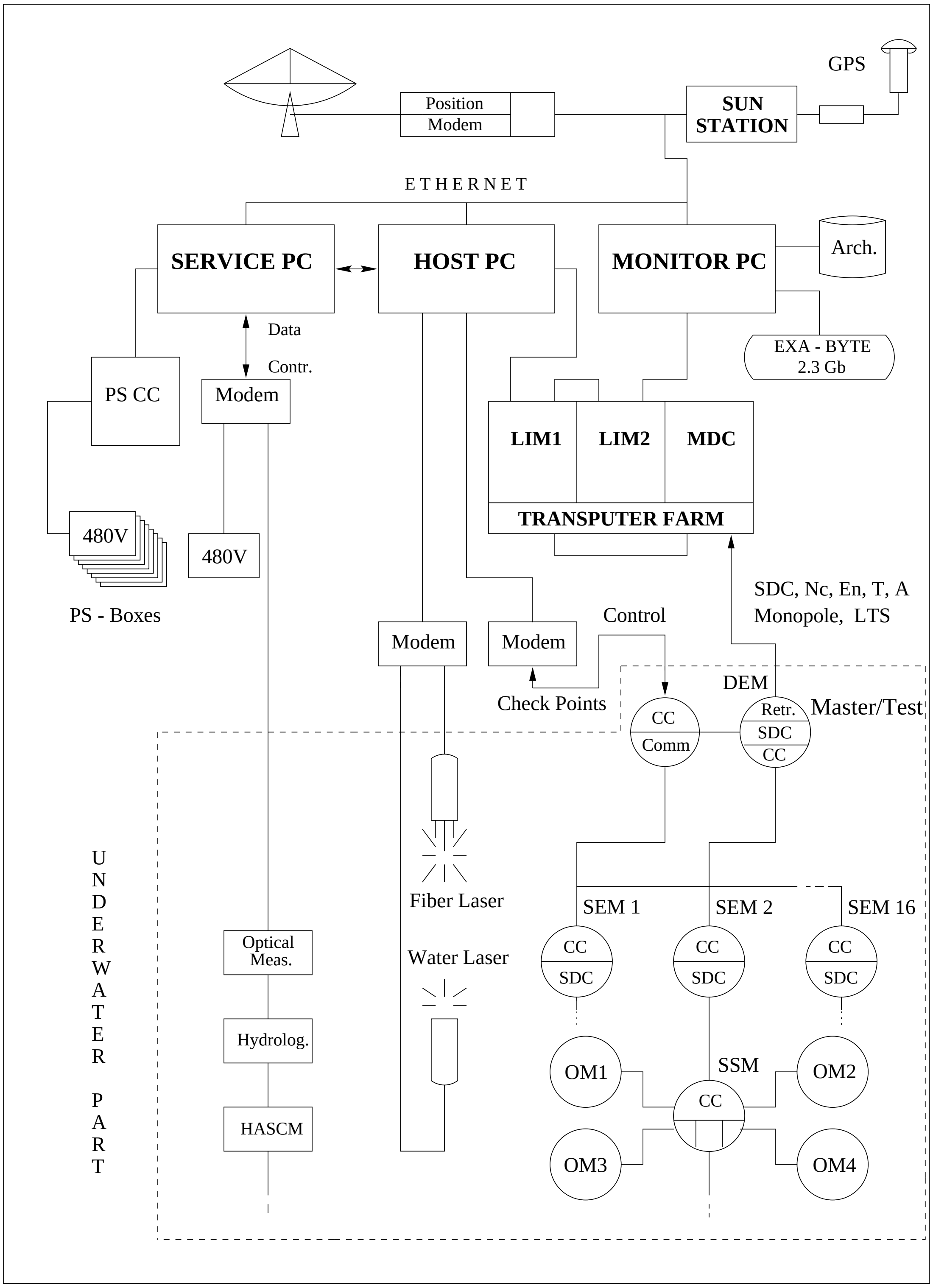

Figure 12: Sketch of the NT–200 *DAQ system*. The underwater electronics is only partly shown. For the abbreviations see the text.

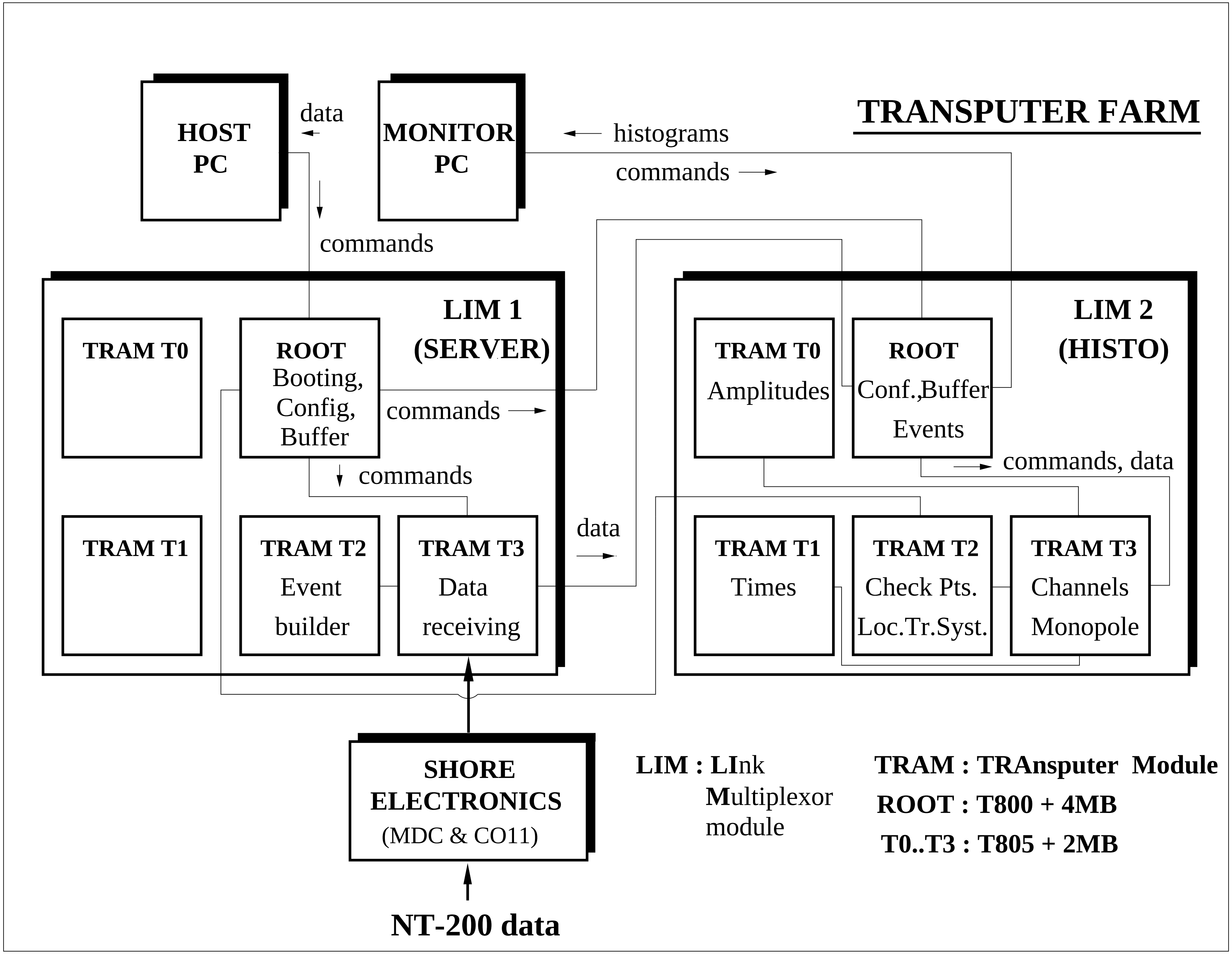

Figure 13: Block diagram of the *Transputer Farm*.

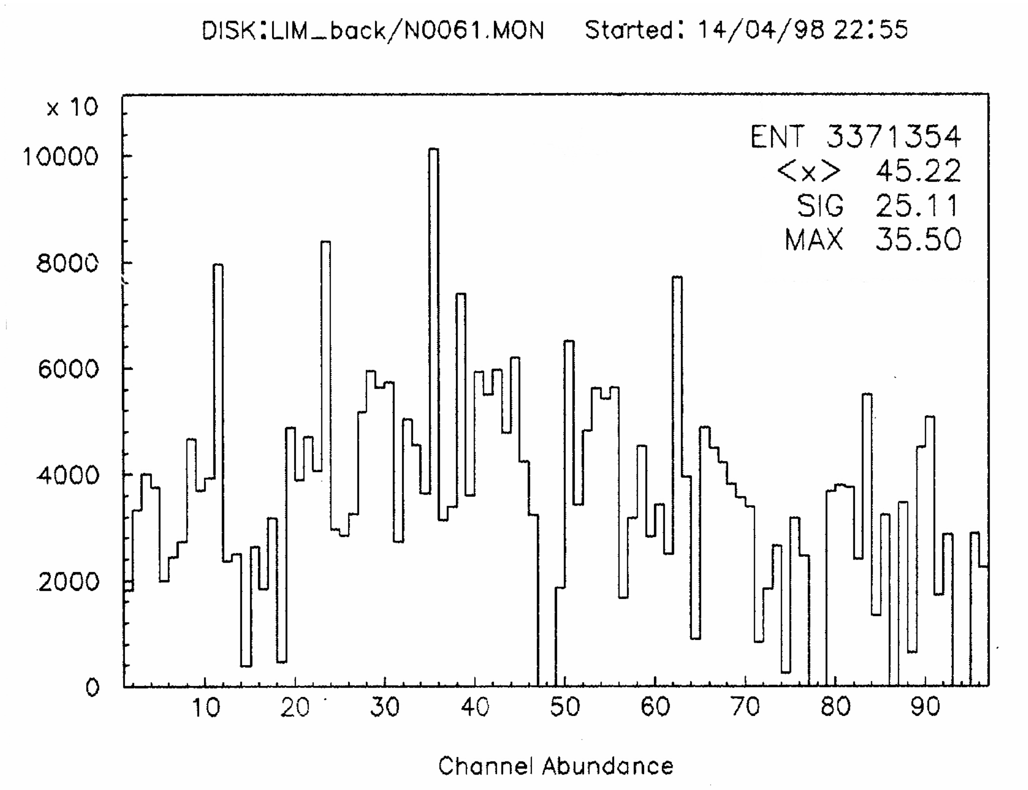

Figure 14: Monitorogram of NT–200 channel abundance.

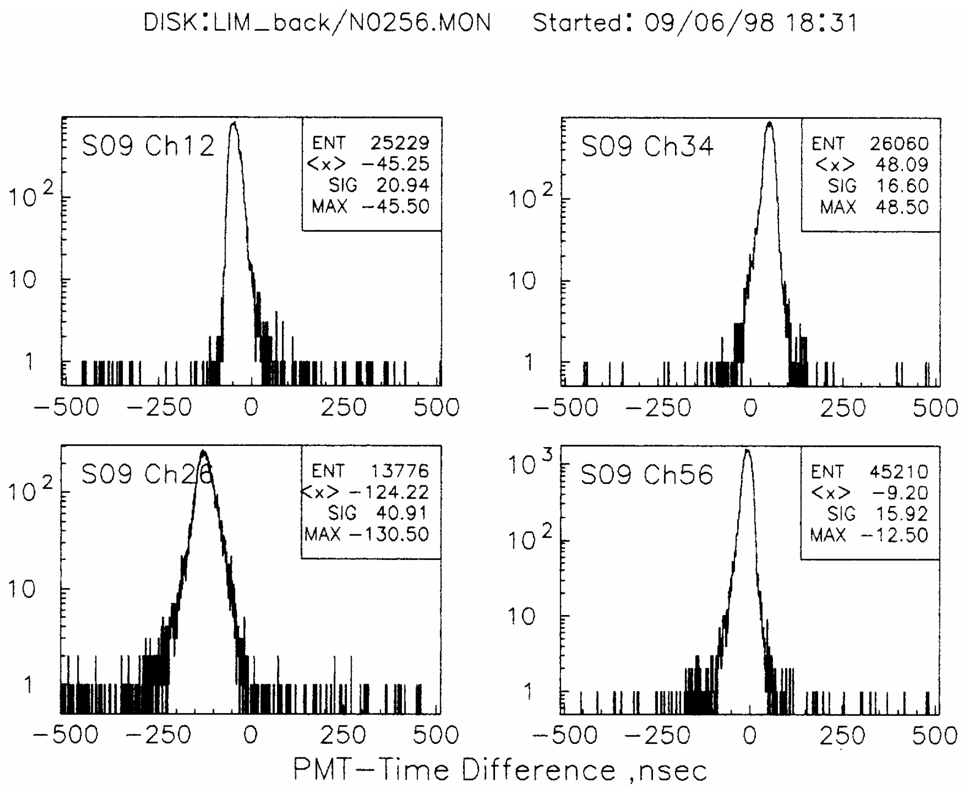

Figure 15: Time difference distribution monitorogram for 6 channels of the top half of NT–200 central string (Half-string 9). Channel 2 is upward faced. Calibration time scale factors were used for timing transformation (without individual time shifts).

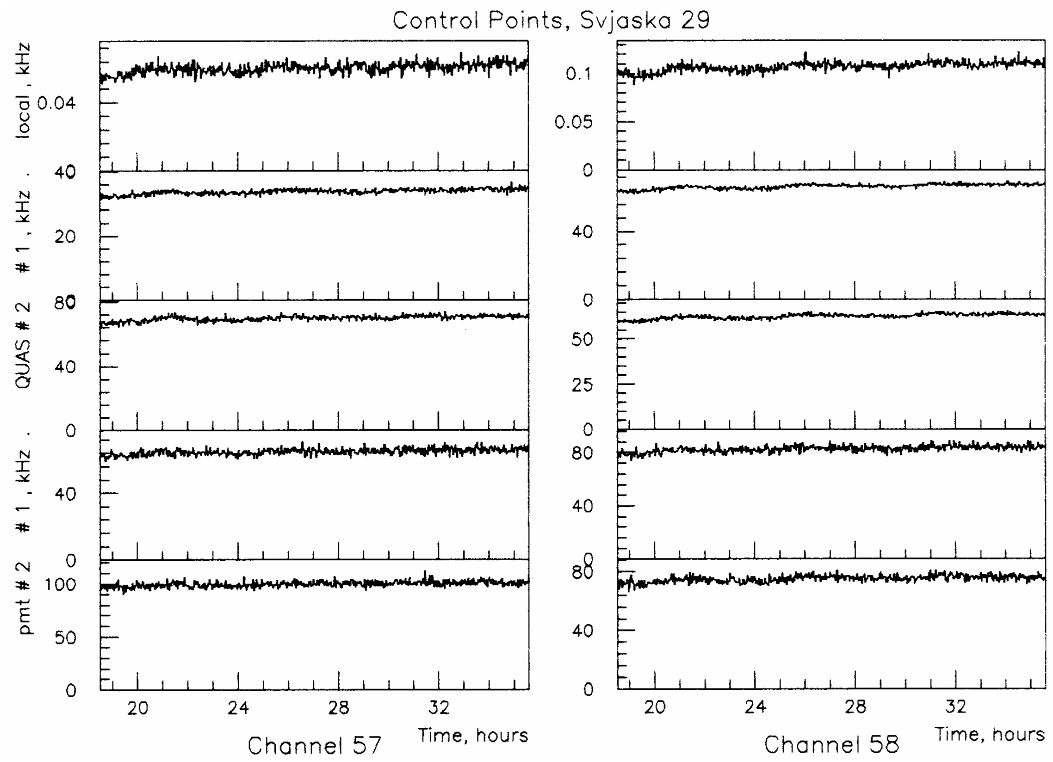

Figure 16: The Check Point real-time monitorogram for Svjaska System Module # 29 over 16 hours of NT-200 operation. The counting rates for all 4 small PMTs (pmt), big photocathodes (QUAS) and 2 local triggers (loc) are shown (in kHz). The period of Check Point data taking was about 2 min.

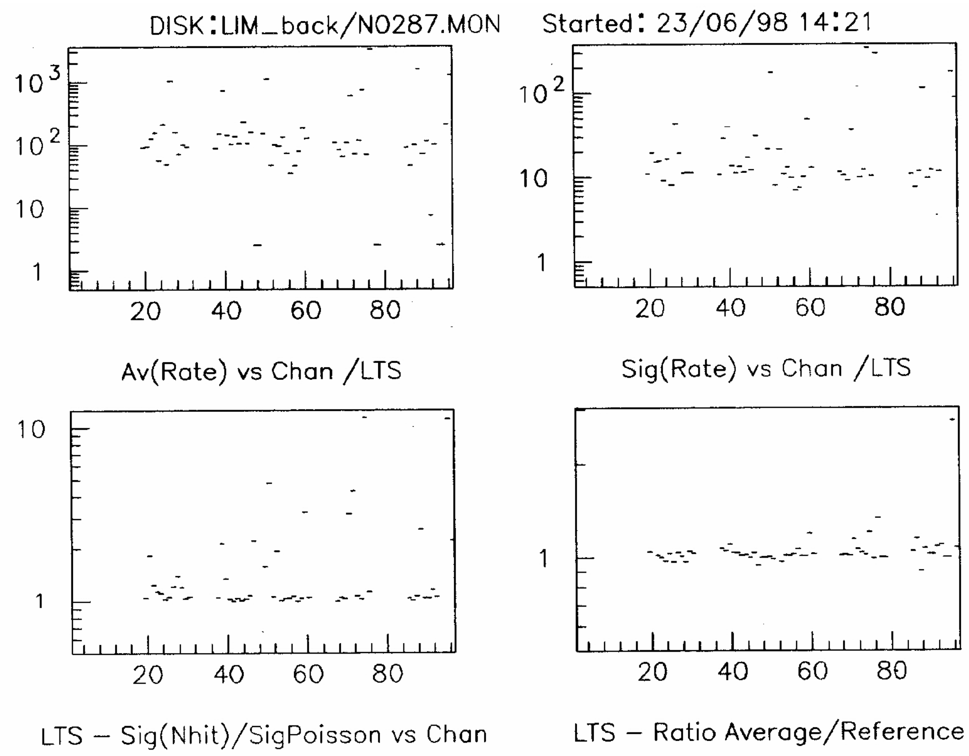

Figure 17: Local Trigger System (LTS) monitoring display (see text). *Chan* denotes the channel number.